

Physics-Informed Neural Network for Online State of Health Estimation of Lithium-ion Batteries

Fusheng Jiang

School of Reliability and Systems Engineering, Beihang University, China. E-mail: jiangfusheng@buaa.edu.cn

Yi Ren

School of Reliability and Systems Engineering, Beihang University, China. E-mail: renyi@buaa.edu.cn

Xianghong Liu

Troops 93160, China. E-mail: liuxh232@163.com

Quan Xia

School of Reliability and Systems Engineering, Beihang University, China. E-mail: quanxia@buaa.edu.cn

Dezhen Yang

School of Reliability and Systems Engineering, Beihang University, China. E-mail: dezhenyang@buaa.edu.cn

Cheng Qian

School of Reliability and Systems Engineering, Beihang University, China. E-mail: cqian@buaa.edu.cn

Zili Wang

School of Reliability and Systems Engineering, Beihang University, China. E-mail: wzl@buaa.edu.cn

Sifeng Bi

Department of Mechanical and Aerospace Engineering, Glasgow, UK. E-mail: sifeng.bi@strath.ac.uk

This paper presents a novel approach for estimating the state of health (SOH) of lithium-ion batteries, which addresses the challenge of being unable to measure the internal cell temperature during operation. The proposed approach, termed physics-informed neural network (PINN), integrates prior physical knowledge with measurable actual data to estimate the SOH of the batteries. To achieve this, an equivalent circuit model is established to characterize the electrical behavior characteristics of the batteries. An electric-thermal partial differential equation is also set to describe the batteries' heat generation mechanism and heat transfer process, and the batteries' instantaneous temperature field is reconstructed based on the PINN model. Finally, the online estimation of the lithium-ion batteries SOH is realized using the piecewise Arrhenius model. The simulation and experimental results show that the proposed approach achieves an average error of 0.37% in the temperature field reconstruction of the lithium-ion batteries and an average error of 0.15% in the online SOH estimation, even when the internal cell temperature cannot be measured.

Keywords: Physics-informed neural network, SOH estimation, Temperature field reconstruction, Arrhenius model, Cycle degradation.

1. Introduction

Clean energy instead of traditional petroleum resources can effectively avoid the increasingly

severe environmental pollution problem. Lithium-ion batteries have been widely adopted as necessary energy storage and supply components

because of their advantages, such as high specific energy, long cycle life, and low self-discharge rate (Gao D et al. 2020). Therefore, accurate and fast online estimation of the health condition of lithium-ion batteries is a critical task.

Numerous studies have focused on estimating the state of health (SOH) of lithium-ion batteries, which can be divided into two main categories: mode-driven methods and data-driven methods. Commonly used model-driven methods include the P2D model (Wild M et al. 2015), electrochemical impedance model, LPM model, Thevenin model, RC model, and PNGV model (Gaddam RR et al. 2021). Gao R J et al. (2022) measured the structural parameters of lithium-ion batteries using a scanning electron microscope. Then they proposed a health status estimate based on the P2D model of the lithium-ion batteries cell. Similarly, Lee et al. (2012) evaluated the SOH of the batteries based on the batteries' terminal voltage, load current, and polarization impedance electrochemical model from the perspective of macroscopic battery parameters using the porous electrode theory. Furthermore, some scholars (Jaguemont J et al. 2016 and Prasad G K et al. 2013) have used simplified electrochemical models to estimate lithium-ion batteries' SOH and remaining useful life (RUL).

In recent years, the application of data-driven methods has attracted significant attention due to the increasing maturity of machine learning and big data technologies. Some researchers have exploited convolutional neural networks and long short-term memory neural networks to extract and model the characteristics of lithium-ion batteries charging voltage data, leading to the estimation of battery capacity degradation (Chen Z et al. 2022). Other researchers have used a double-layer Bi-LSTM neural network to model NASA's public lithium-ion batteries capacity degradation data and evaluate the batteries' SOH and Remaining Useful Life (RUL) (Wang Y et al. 2021).

Physics-informed Neural Network (PINN) is a data model fusion deep learning framework for solving supervised learning tasks, which is widely used to solve forward and backward problems of partial differential equations (Raissi M et al. 2019). The partial differential equations are integrated into the training process of neural networks as constraints, thereby improving neural network robustness and interpretability. In this paper, we proposed an online estimation of SOH using the internal temperature of the batteries

during operation. It combined the heat generation and heat transfer models with measurement data to estimate the SOH of lithium-ion batteries, thus reducing the need for measurement data.

2. Lithium-ion battery electric-thermal model

2.1. Equivalent circuit model

An equivalent circuit model can describe lithium-ion batteries' capacitive and resistive characteristics under the charging and discharging phases. The widely accepted second-order RC equivalent circuit model (ECM) was chosen for this study. A schematic representation of the primary circuit structure is provided in Fig. 1.

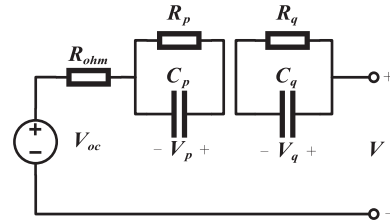


Fig. 1. Lithium-ion battery second-order RC equivalent circuit model.

The mathematical formula presented below expresses the equivalent circuit model depicted in Fig.1 by Kirchhoff's law:

$$\begin{cases} U = E_0 - V_p - V_q - IR_{ohm} \\ I = \frac{V_p}{R_p} + C_p \frac{dV_p}{dt} \\ I = \frac{V_q}{R_q} + C_q \frac{dV_q}{dt} \end{cases} \quad (1)$$

where E_0 is the open circuit voltage, which is equivalent to an ideal DC voltage source; R_{ohm} is the internal ohmic resistance of the batteries; U is the working voltage of the lithium-ion batteries; R_p and R_q are the electrochemical polarization resistance and the concentration difference polarization resistance, respectively; V_p and V_q are electrochemical polarization voltage and concentration difference polarization voltage respectively; C_p and C_q are electrochemical polarization capacitance and concentration difference polarization capacitance respectively.

To achieve parameter identification of this equivalent circuit and obtain model parameters that accurately reflect the batteries' behavior, it is necessary to transform Eq.(1) into a discrete form. The discretization process of the polarization voltage V_p and the concentration difference

polarization voltage V_q is the same, and the discrete state space model can be expressed as:

$$\begin{cases} U_k = E_{0,k} - V_{p,k} - V_{q,k} - I_k R_{ohm} \\ V_{p,k+1} = e^{-\frac{t}{R_p C_p}} V_{p,k} + I_k R_p \left(1 - e^{-\frac{t}{R_p C_p}}\right) \\ V_{q,k+1} = e^{-\frac{t}{R_q C_q}} V_{q,k} + I_k R_q \left(1 - e^{-\frac{t}{R_q C_q}}\right) \end{cases} \quad (2)$$

where $V_{p,k+1}$ and $V_{q,k+1}$ represent the electrochemical polarization voltage and concentration difference polarization voltage of the lithium-ion batteries at time $k+1$, respectively; $E_{0,k}$ represents the open circuit voltage of the lithium-ion batteries at time k , which is influenced by the state of charge (SOC).

The relationship between open circuit voltage (OCV) and SOC can be fitted using the experimental data, expressed as follows:

$$E_0 = \sum_{i=0}^n k_i SOC^i \quad (3)$$

where n signifies the polynomial order, where a higher value indicates a more extraordinary representation ability of the model; k_i is the polynomial coefficient derived through the fitting process.

2.2. Electric-thermal coupling model

In this paper, the widely accepted Bernardi model (Bernardi D et al. 1985) was used to calculate the total internal heat generation during the operation. Based on the principle of energy conservation, the expression of the heat generation model in the batteries is as follows:

$$Q_{cell} = \frac{I}{V_b} \left[(U - E_0) + T \frac{\partial E_0}{\partial T} \right] \quad (4)$$

where Q_{cell} is the total heat output of the batteries; V_b is the volume of the batteries cell; U is the working voltage of the batteries; E_0 is the open circuit voltage of the batteries; T is the thermodynamic temperature, where $\partial E_0 / \partial T$ is the temperature coefficient of the batteries voltage with temperature.

By Fourier's law, the heat conduction equation within the batteries in the characteristic direction x is expressed as follows:

$$q = -\lambda \frac{\partial T}{\partial x} \quad (5)$$

where q is the heat flux per unit area; λ is the heat transfer coefficient per unit area; T is the temperature; x represents the direction.

The heat transfer model of lithium-ion batteries can be expressed by the energy conservation equation (Li W et al. 2021):

$$\rho C_p \frac{\partial T}{\partial t} + \nabla \cdot (-\lambda \nabla T) = Q_{cell} \quad (6)$$

where ρ is the density; C_p is the heat capacity at constant pressure; T is the thermodynamic temperature; λ is the thermal conductivity.

3. SOH estimation method based on PINN

This section is dedicated to the proposed PINN-based method for estimating the state of health (SOH) of lithium-ion batteries online, and the methodology is presented in Fig. 2.

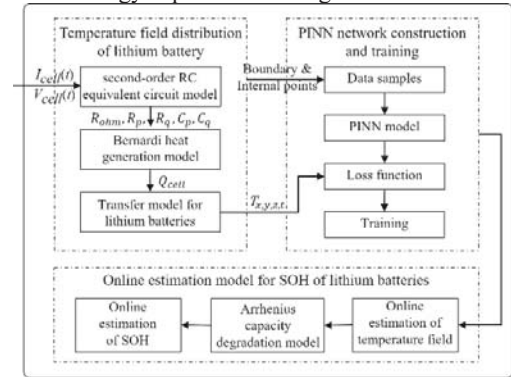


Fig. 2. The PINN-based online estimation method flow of SOH.

3.1. Parameter Identification of Equivalent Circuit Model Based on RLS

This study employed the recursive least squares (RLS) method to implement the parameter identification of the second-order RC ECM. The corresponding calculation expression is as follows:

$$\begin{cases} \hat{\theta}(k) = \hat{\theta}(k-1) + K(k)[y(k) - \psi(k)\hat{\theta}(k-1)] \\ K(k) = \frac{P(k-1)\psi(k)}{1 + \psi^T(k)P(k-1)\psi(k)} \\ P(k) = [I - K(k)]\psi^T(k)P(k-1) \end{cases} \quad (8)$$

where $\hat{\theta}$ is the parameter identification value of the lithium-ion batteries equivalent circuit model; K is the algorithm gain; P is the state estimation covariance matrix; y is the output of the lithium-ion batteries, that is, the measured voltage; ψ is the experimental data matrix; I is the identity matrix.

3.2. Temperature field reconstruction based on PINN

In this section, we reconstructed the internal temperature field distribution during the charging and discharging process of the lithium-ion batteries

based on PINN. The structure of the proposed model is illustrated in Fig. 3.

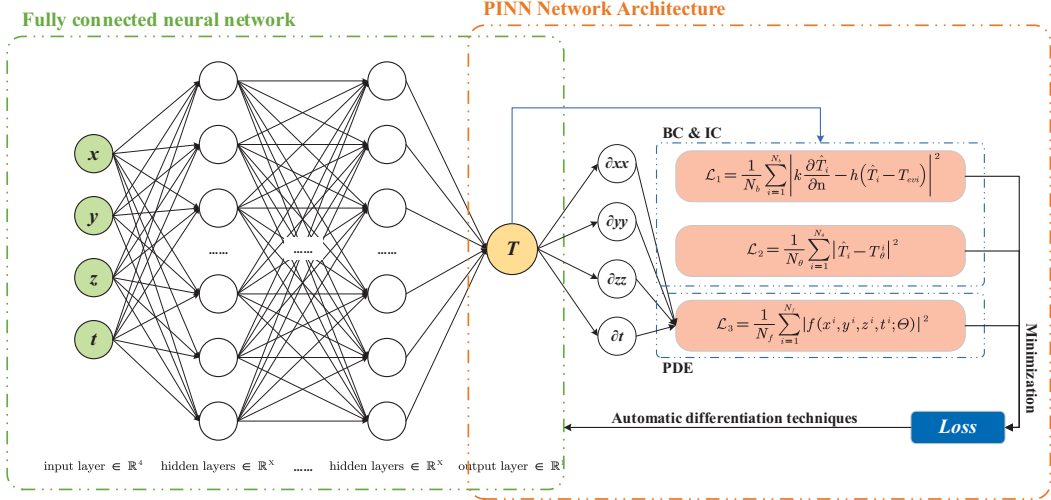


Fig. 3. Architecture flow of the PINN model

The initial step involves using the input parameters to construct a deep fully connected neural network. The nonlinear functional relationship between the input features (x, y, z, t) and the output feature T was determined by fitting the Artificial Neural Network (ANN). The corresponding expression is presented below:

$$\hat{T} = ANN(x, y, z, t; \theta) \quad (8)$$

The output of the ANN model is automatically differentiated, and the residual function of PINN is defined as $f(x, y, z, t; \theta)$ according to Eq.(6), and its expression is as follows:

$$f(x, y, z, t, \theta) = \rho C_p \frac{\partial T}{\partial t} - \nabla(\lambda \nabla T) - Q_{cell} + Q' \quad (9)$$

In this study, the mean square error (MSE) is utilized to construct the loss function of PINN model. The expressions for these error components are as follows:

$$MSE_{total} = \alpha MSE_{ANN} + \beta MSE_{PINN} \quad (10)$$

$$MSE_{ANN} = \underbrace{\frac{1}{N_b} \sum_{i=1}^{N_b} \left| k \frac{\partial \hat{T}_i}{\partial n} - Ah(\hat{T}_i - T_{env}) \right|^2}_{MSE_{BC}} \quad (11)$$

$$+ \underbrace{\frac{1}{N_\theta} \sum_{i=1}^{N_\theta} |\hat{T}_i - T_{\theta,i}|^2}_{MSE_{IC}}$$

$$MSE_{PINN} = \frac{1}{N_f} \sum_{i=1}^{N_f} |f(x^i, y^i, z^i, t^i; \theta)|^2 \quad (12)$$

where MSE_{ANN} is the average error loss of the data-driven item; MSE_{PINN} is the average error loss of the physical information-driven item; α is the weight of the error loss of the data-driven item; β is the weight of the error loss of the physical information-driven item; MSE_{BC} is the data-driven item medium boundary condition average error loss; MSE_{IC} is the initial condition average error loss in the data-driven item; N_b , N_θ , and N_f represent the boundary sampling points, initial sampling points, and configuration training set sampling points in turn.

3.3. Online SOH estimation based on the Arrhenius model

In this paper, we concentrated on the capacity fading of lithium-ion batteries, and the mathematical expression for defining the SOH of lithium-ion batteries is presented below:

$$SOH = \left(1 - \frac{C_{fade}}{C_{nom}}\right) \cdot 100\% \quad (13)$$

where C_{nom} is the rated capacity of the batteries under certain conditions, and C_{fade} is the fading capacity of the batteries.

The rate of different electrochemical reactions occurring inside the batteries fluctuates with temperature. The relationship between battery capacity degradation and temperature is by Arrhenius' law (Wang J et al. 2011) under the

temperature range of 288.15 K to 333.15 K. The mathematical formula of the capacity degradation model can be expressed as follows:

$$C_{fade} = \sum_{i=0}^N \int_0^t A \cdot \exp\left(-\frac{E_a}{RT_i(t)}\right) \cdot N_i dt \quad (14)$$

where C_{fade} is the cumulative capacity degradation; N is the number of charging and discharging cycles; t is the charging and discharging cycle time; A is the pre-exponential factor; E_a is the activation energy, 8.314J/(mol·K); $T(t)$ is the temperature.

4. Verification and analysis

4.1. Lithium-ion battery performance and degradation test experiment

In order to assess the effectiveness, accuracy, and generalizability of the method proposed in this study, three independent 18650 LiFePO4 power batteries were utilized to conduct hybrid pulse power characterization (HPPC) and battery degradation experiments. The rated capacity and voltage of the lithium-ion batteries were 1400mAh and 3.2V, respectively.

To enable the dynamic evaluation of the electrical performance of the lithium-ion batteries during the entire life cycle of lithium-ion batteries degradation, this study conducted HPPC experiments during the lithium-ion batteries degradation experiments. It collected voltage and current data every 30s.

With the #1 battery as an example, Fig. 4 depicts the current and voltage variation of the batteries during the HPPC. Fig. 5 and Fig. 6 show the voltage and current variation of the batteries during the degradation experiment, respectively.

4.2. Evaluation metrics

To evaluate the effectiveness and accuracy of the proposed method, root mean square error (RMSE) and mean absolute percentage error (MAPE) were used as evaluation metrics in this study. The calculation formulas for the above-mentioned evaluation metrics are as follows:

$$RMSE = \sqrt{\frac{1}{n} \sum_{i=1}^n (y_i - \hat{y}_i)^2} \quad (15)$$

$$MAPE = \sum_{i=1}^n \left| \frac{\hat{y}_i - y_i}{y_i} \right| \cdot \frac{100\%}{n} \quad (16)$$

where y_i is the real value; \hat{y}_i is the estimated value; n is the number of samples.

4.3. PINN temperature field model verification

To validate the accuracy of the proposed PINN model, the charging and discharging process measured data and temperature distribution simulation results of the #1 lithium-ion battery were selected for comparison.

Using the results obtained from internal resistance identification, the temperature field distribution while charging the #1 battery was simulated by implementing COMSOL 5.6 software. A time-varying function was established to represent the heat generation by integrating the internal resistance identification and calculating the heat generation model.

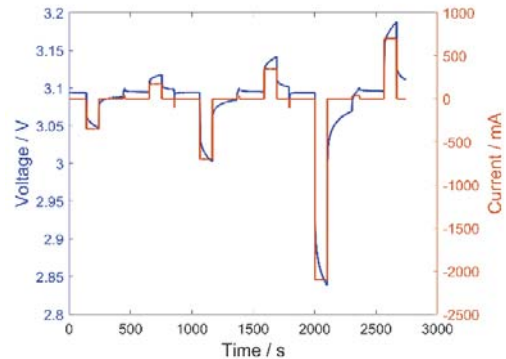


Fig. 4. Lithium-ion battery HPPC experiment cycle test curve.

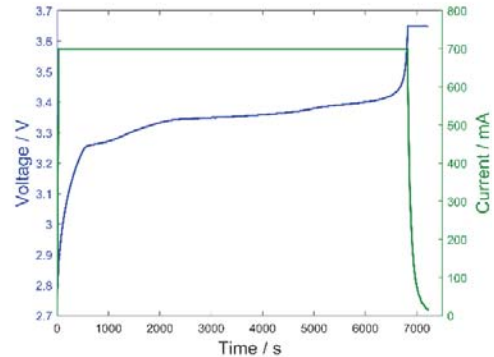


Fig. 5. Lithium-ion battery degradation test charging cycle curve.

The training set data utilized in this study was derived from the calculation results of the COMSOL 5.6 simulation software. The Latin hypercube sampling method was used to generate 200 sets of samples for the batteries boundary, with the initial condition sampling point being 100 sets of samples. The MSE_{PINN} value was calculated from a total of 20,000 sets of global sampling coordinate points. The hyperparameters for the constructed PINN model are presented in Table 1.

The temperature change curve of the #1 lithium-ion batteries charging process was compared to the COMSOL temperature field simulation results at $t=7000s$, as shown in Fig. 7.

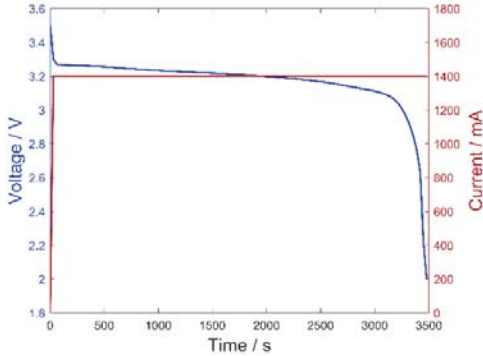


Fig. 6. Lithium-ion battery degradation test discharge cycle curve.

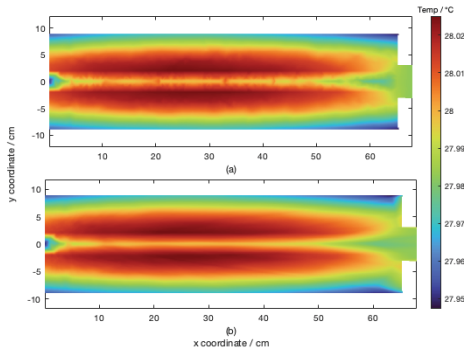


Fig. 7. Comparison of PINN model and COMSOL simulation temperature field reconstruction results at $t = 7000s$: (a) COMSOL simulation results; (b) PINN model results.

The analysis of the results presented in Fig. 7 indicates that the PINN model, trained using both measured and simulated data, exhibits a strong ability to represent the temperature field. The RMSE error in the entire domain is 0.17%, and the MAPE error is 0.37%.

Table 1. Hyperparameters of PINN mode

Hyperparameters	Value
Neuron structure	[4, 200, 200, 200, 200, 1]
Activation function	Sigmoid
Optimizer	Adam
Learning rate	0.0001
Iterations	20000
Weight initialization	Xavier

The temperature change values of the cylindrical temperature side surface of the #1 battery were collected during charging to verify the accuracy of the COMSOL simulation results and the PINN model, and the results are shown in Fig. 8.

By analyzing the results depicted in Fig. 7 and Fig. 8, the proposed PINN model constructed based on the simulated data shows high performance. Compared with the COMSOL simulation method, the PINN model maintains the same estimation accuracy while requiring less computational cost and can be re-trained during the operation process based on the measured temperature values, which results in more suitable for online applications.

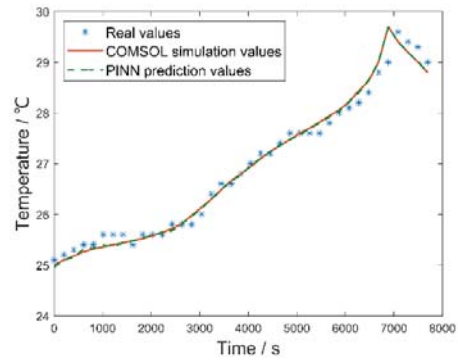


Fig. 8. PINN Model Estimating Temperature Results of Lithium-ion Battery Charging Process.

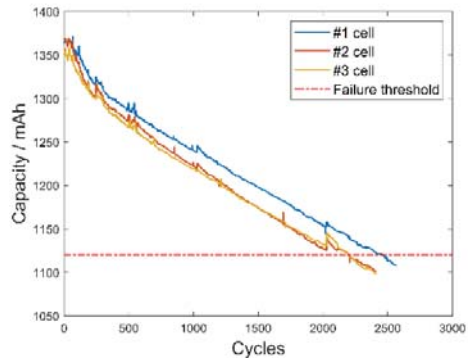


Fig. 9. Lithium-ion batteries capacity degradation trajectory curve.

As we all know, online application methods often need to make a trade-off between accuracy and computational cost. Simulation methods are often used in ideal conditions without considering data noise, while the PINN model is essentially a data-driven method with good nonlinear expression capabilities. It can show similar result accuracy for

low-quality data samples and has stronger robustness.

4.4. Lithium-ion battery SOH online estimation results

This section presents the experimental verification of the proposed online SOH estimation method using measured data of capacity degradation from three lithium-ion batteries labeled #1, #2, and #3. The overall capacity degradation trajectory is presented in Fig. 9. This section analyses the characteristics of the capacity data of lithium-ion battery degradation experiments. It divides the overall degradation process of lithium-ion batteries into four stages. The Arrhenius model with variable parameters is used to estimate the SOH for each stage to increase the characterization ability of the model. The multi-stage parameters and error results of batteries #1, #2, and #3 are shown in Table 2, and the overall SOH estimation results for each battery are illustrated in Fig. 10 to Fig. 12.

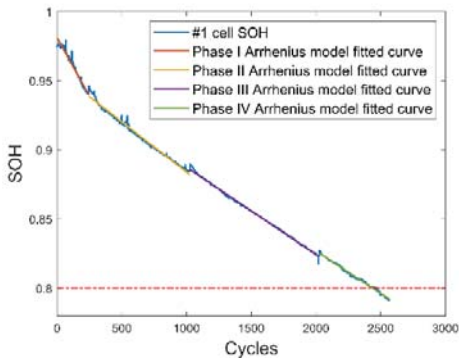


Fig. 10. #1 Lithium-ion battery Arrhenius model online estimation results.

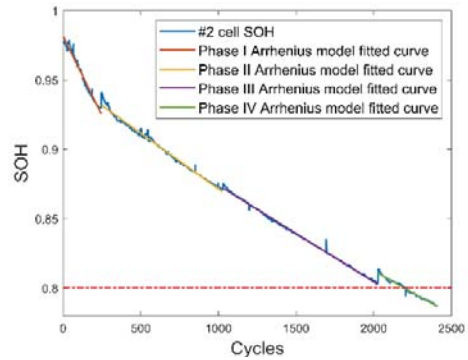


Fig. 11. #2 Lithium-ion battery Arrhenius model online estimation results.

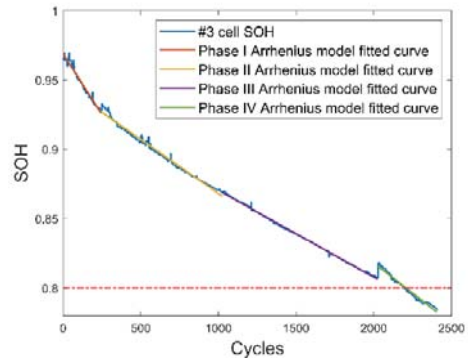


Fig. 12. #3 Lithium-ion battery Arrhenius model online estimation results.

Table 2. The parameters identification results of the Arrhenius model and corresponding estimation errors.

Cycle range	No.	E_a	A	RMSE	MAPE
The first stage (1~245 times)	#1	12104.604	2.294	0.21%	0.160
	#2	10772.694	1.345	0.24%	0.206
	#3	14811.463	6.788	0.19%	0.144
The second stage (250~1025 times)	#1	3959.777	0.130	0.18%	0.153
	#2	3829.609	0.123	0.19%	0.147
	#3	3308.410	0.100	0.20%	0.173
The third stage (1030~2025 times)	#1	3823.996	0.139	0.09%	0.074
	#2	4187.920	0.162	0.08%	0.075
	#3	4553.814	0.187	0.07%	0.065
The fourth stage (2030~EOF times)	#1	10121.675	1.044	0.09%	0.098
	#2	12702.856	2.939	0.11%	0.104
	#3	13858.465	4.672	0.18%	0.189

As indicated in Table 3 through RMSE and MAPE results, the proposed method in this study demonstrates high accuracy and exhibits robust

online SOH estimation capabilities under specific incomplete data conditions.

Table 3. Online estimation error of the SOH of lithium-ion batteries.

Batteries number	RMSE (%)	MAPE (%)
#1	0.14	1.113
#2	0.15	1.562
#3	0.15	1.761

5. Conclusion

This paper presents an online SOH estimation method based on a physical information neural network for lithium-ion batteries. The proposed method addresses the challenging SOH estimation problem in situations where monitoring the internal cells of the batteries is not feasible due to incomplete data. The effectiveness of the proposed method is demonstrated through simulation and experiment using three 18650-type LiFePO₄ power batteries. The simulation and experimental results demonstrated that the proposed method has a high accuracy rate, with an average root mean square error (RMSE) of SOH estimation at 0.15% and an average mean absolute percentage error (MAPE) at 1.48%.

Acknowledgment

This work was supported by the Project of International Cooperation and Exchanges NSFC (No.52311530092), the National Natural Science Foundation of China (NSFC, No.52075028), the Royal Society International Exchanges 2022 Cost Share (NSFC) (Grant Ref IEC\NSFC\223035), and the Project funded by China Postdoctoral Science Foundation 2021M690298.

References

- Gao, Diyu, Yong Zhou, Tianzhen Wang, and Yide Wang (2020). A method for predicting the remaining useful life of lithium batteries based on particle filter using Kendall rank correlation coefficient. *Energies*, 13, 4183.
- Wild, M., L. O'Neill, T. Zhang, R. Purkayastha, G. Minton, M. Marinescu, and G. J. Offer (2015). Lithium-ion sulfur batteries, a mechanistic review. *Energy & Environmental Science*, 8(12), 3477-94.
- Gaddam, Rohit Ranganathan, Leon Katzenmeier, Xaver Lamprecht, and Aliaksandr S. Bandarenka (2021). Review on physical impedance models in modern batteries research. *Physical Chemistry Chemical Physics*, 23(23):12926-44.
- Gao, R. J., ZQ LV, S. Zhao, and X. G. Huang (2022). Health State Estimation of Li-Ion Batteries Based on Electrochemical Model. *Transactions of Beijing Institute of Technology*, 645:1-7.
- Lee, James L., Andrew Chemistruck, and Gregory L. Plett (2012). One-dimensional physics-based reduced-order model of lithium dynamics. *Journal of Power Sources*, 220, 430-448.
- Jagemont, Joris, Loïc Boulon, and Yves Dubé (2016). Characterization and Modeling of a Hybrid-Electric-Vehicle Lithium Batteries Pack at Low Temperatures. *IEEE Transactions on Vehicular Technology*, 65, 1-14.
- Prasad, Githin K., and Christopher D. Rahn (2013). Model-based identification of aging parameters in lithium-ion batteries. *Journal of power sources*, 232, 79-85.
- Chen Z, Li J Y, Shu X (2022). State of Health Estimation for Lithium Batteries Based on Hybrid Neural Network. *Journal of Kunming University of Science and Technology (Natural Sciences)*, 47(3):87-96.
- Wang Y, Liu X, Gao D X (2021). The SOH estimation and RUL prediction of lithium-ion batteries based on BiLSTM. *Electronic Measurement Technology*, 44(20):1-5.
- Raissi, Maziar, Paris Perdikaris, and George E. Karniadakis (2019). Physics-informed neural networks: A deep learning framework for solving forward and inverse problems involving nonlinear partial differential equations. *Journal of Computational physics*, 378:686-707.
- Bernardi, D., E. Pawlikowski, and John Newman (1985). A general energy balance for batteries systems[J]. *Journal of the electrochemical society*, 132(1):5.
- Javani, Nader, I. Dincer, G. F. Naterer, and B. S. Yilbas (2021). Simulation Analysis of Heat Transfer in Cooling System of Li-ion Batteries Pack for Vehicles. *Equipment Environmental Engineering*, 18(2): 6-12.
- Wang, John, Ping Liu, Jocelyn Hicks-Garner, Elena Sherman, Souren Soukiazian, Mark Verbrugge, Harshad Tataria, James Musser, and Peter Finamore (2011). Cycle-life model for graphite-LiFePO₄ cells. *Journal of power sources*, 196(8):3942-3948.